A simple solvothermal synthesis of MFe$_2$O$_4$ (M=Mn, Co and Ni) nanoparticles

S. Yáñez-Vilar[a], M. Sánchez-Andújar[a], C. Gómez-Aguirre[a], J. Mira[b], M.A. Señarís-Rodríguez[a], S. Castro-García[a, ,]

a Departamento de Química Fundamental, Facultade de Ciencias, Universidade da Coruña, A Zapateira s/n, 15071 A Coruña, Spain

b Departamento de Física Aplicada, Universidade de Santiago de Compostela, 15782 Santiago de Compostela, Spain

## Abstract

Nanoparticles of MFe$_2$O$_4$ (M=Mn, Co and Ni), with diameters ranging from 5 to 10 nm, have been obtained through a solvothermal method. In this synthesis, an alcohol (benzyl alcohol or hexanol) is used as both a solvent and a ligand; it is not necessary, therefore, to add a surfactant, simplifying the preparation of the dispersed particles. We have studied the influence of the synthetic conditions (temperature, time of synthesis and nature of solvent) on the quality of the obtained ferrites and on their particle size. In this last aspect, we have to highlight that the solvent plays an important role on the particle size, obtaining the smallest diameters when hexanol was used as a solvent. In addition, the magnetic properties of the obtained compounds have been studied at room temperature (RT). These compounds show a superparamagnetic behaviour, as

was expected for single domain nanoparticles, and good magnetization values. The maxima magnetization values of the MFe$_2$O$_4$ samples are quite high for such small nanoparticles; this is closely related to the high crystallinity of the particles obtained by the solvothermal method.

Graphical abstract

An adaptation of the solvothermal method allow us to obtain stable suspensions of monodispersed particles
of MFe$_2$O$_4$ (M=Mn, Co and Ni), with diameters ranging from 5 to 10 nm, and with good crystallinity.
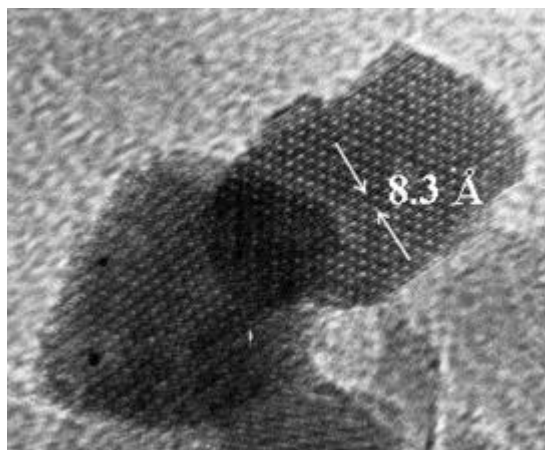
Keywords

1. Introduction

The synthesis of nanostructured magnetic materials has become an important area of research and is attracting growing interest, not only in answering basic research questions, but also in technological applications and in biosciences [1], [2], [3] and [4]. In particular, the nanometer-scale MFe$_2$O$_4$ (M=Mn, Fe, Co, Ni,…) spinel ferrites and their dispersions in various substances are among the most important magnetic materials, which have been widely used for studies of nanomagnetism and have shown great potential for important technological applications in many fields such as high-density information storage, ferrofluids, colour imaging, catalysis, biomolecule separation, medical diagnosis, drug delivery and so forth[5], [6], [7], [8], [9], [10], [11], [12], [13] and [14].

It is well known that the magnetic and electrical properties of MFe$_2$O$_4$ nanoparticles can be varied by changing the identity of the divalent M^{2+} cation or by partial substitution, while maintaining the basic crystal structure. Additionally, the magnetic properties of the nanoparticles are strongly dependent on their shape, size and crystallinity. To use MFe$_2$O$_4$ ferrites for future magnetic nanodevices and biomedical applications, size-tuned ferrite particles with diameters ranging from the superparamagnetic threshold at room temperature of <10 nm to the critical single-domain size of 70 nm are needed [15], [16] and [17]. For many of the applications, such as magnetic carriers in bioscience, their size is limited to a very narrow margin of values (from 5 to 10 nm) in order to attain a compromise between magnetic moment and absence of magnetic memory: superparamagnetic particles must be smaller than 10 nm, but their magnetic moment decreases drastically below about 5 nm [18].

Many investigations have been focused until now, not only on the controlled synthesis of ferrite nanoparticles, but also on the correlation between their magnetic properties and either the particulate properties and/or the synthetic conditions [7], [11], [19], [20], [21], [22], [23], [24], [25], [26], [27] and [28]. Although significant progress has been made in this respect, systematic and profound understanding remains challenging, which justifies any effort to find a simple and cost-effective way for the production of sized-tuned monodisperse nanoparticles [29].

Techniques such as sol–gel [30], coprecipitation [31], [32] and [33], mechanochemical processing [34] and [35], microemulsion [26], [36] and [37] and microwaves [38] have been commonly used to prepare ferrite nanoparticles. But, until now, the most economical ways for the production of large quantities of nanosized ferrite particles are chemical precipitation [39] and solvothermal synthesis [11], [19], [40], [41] and [42]. In general, solvothermal synthesis offers many advantages over other methods, such as its simplicity, the high crystallinity of the obtained products at relatively low temperature ($T \sim 180$ °C), the capability to control crystal growth and its adequacy for the preparation of large quantities of samples. Hydrothermal synthesis—a specific solvothermal method where water is employed as a solvent—has been employed since the end of the 19th century for the synthesis of different ferrites [43], [44] and [45], but the experimental conditions for these syntheses are sometimes poorly defined [46]. Most of these preparations involve a combination of coprecipitation and hydrothermal synthesis [18]. An innovation to the hydrothermal method is the introduction of microwaves during the hydrothermal synthesis to increase the kinetics of the ferrite particles formation [47]. Another solvothermal synthesis method—in non-aqueous solvent—that has been used to prepare MFe$_2$O$_4$ (M=Fe, Co, Mg, Cu, Ni,

Zn) [48] and [49] ferrites is based on the partial reduction of the reagents by ethylene glycol with the presence of NaAc and polyethylene glycol (PEG). In this so-called polyol process [50] the ethylene glycol serves both as a reducing agent and as a solvent, while NaAc and PEG were used for electrostatic stabilization to prevent particles from agglomeration and as a protective agent respectively. Pinna et al. [51] have recently developed a solvothermal method for the synthesis of metal oxide nanoparticles that employs benzyl alcohol as a solvent and a ligand at the same time, instead of the mixtures of solvents and ligands used before. Therefore, the use of surfactants to prevent agglomeration has been avoided. This solvothermal method simplifies even more the synthesis of the dispersed nanoparticles. In this aspect, we have to highlight the Niederberger works using the benzyl alcohol as a solvent system to prepare nanocrystals of different metal oxides, such as $BaTiO_3$, CeO_2, $NaNbO_3$, etc. [52].

In the present work, we have employed an adaptation of the solvothermal synthesis of Fe_3O_4[50] to prepare single-phase nano-sized MFe_2O_4 (M=Mn, Co and Ni) ferrites, with particle sizes between 5 and 10 nm. We have explored the possibilities of further control of the size and agglomeration of the magnetic ferrite nanoparticles by this method, varying the temperature and time of synthesis, and using two different solvents/ligands: benzyl alcohol and hexanol. In order to improve the magnetic properties of the particles, we have investigated the effects of the synthesis conditions (solvents/ligands, temperature and reaction time) on the size of the nanoparticles and on their saturation magnetization.

2. Experimental

Samples of MFe_2O_4 (M=Mn, Co and Ni) nanoparticles were prepared by the solvothermal method. All the reagents were of analytical grade and were used without any further purification. A typical preparation procedure was as follows: to obtain 0.1 g of ferrite, the required quantities of Mn(acac)$_2$ (Aldrich, technical grade), Co(*acac*)$_2$ (Fluka, 97%) or Ni(*acac*)$_2$ (Aldrich, 90%) were mixed with Fe(*acac*)$_3$ (Aldrich, 97%) and dissolved in benzyl alcohol (Panreac, 98%) or hexanol (Panreac, 98%). The resulting solutions were stirred thoroughly and then transferred into a 23 mL Teflon-lined stainless-steel autoclave to a filling capacity of 40%. The crystallization was carried out under autogenous pressure at temperatures of 180 or 190 °C for 24 or 48 h. All the synthesis conditions (solvents, temperatures and reaction times) used for the preparation of the different MFe_2O_4 samples are summarized in Table 1. Then, the

autoclave was cooled naturally to room temperature, after centrifugation at 5000 rpm for 30 min, the supernatant liquids were discarded and the remaining products were washed thoroughly with ethanol to remove the excess of ligands and air-dried at room temperature.

Table 1. Synthesis conditions and structural and magnetic properties of the $M\text{Fe}_2\text{O}_4$ samples.

Sample	Synthesis conditions: solvent temperature/time	Crystalline phases[a]	$M\text{Fe}_2\text{O}_4$ lattice parameter (Å)[a]	Nanoparticle size (nm)[b]	Magnetization at 10 kOe (emu/g)
Mn-1	Benzyl alcohol 180 °C/24 h	MnFe_2O_4	8.52(24)	7.4±0.8	53.5
Mn-2	Hexanol 180 °C/24 h	MnFe_2O_4	8.52(52)	5.0±0.8	35.1
Co-1	Benzyl alcohol 180 °C/24 h	CoFe_2O_4	8.39(20)	7.6±0.8	56.6
Co-2	Benzyl alcohol 180 °C/48 h	CoFe_2O_4	8.39(03)	8.9±0.6	58.4
Co-3	Benzyl alcohol 190 °C/24 h	CoFe_2O_4	8.39(27)	7.1±1.0	55.4
Co-4	Hexanol 180 °C/24 h	CoFe_2O_4	8.39(18)	5.9±0.6	50.2
Ni-1	Benzyl alcohol 180 °C/24 h	$(\text{Ni}_{1-x}\text{Fe}_x)\text{Fe}_2\text{O}_4+\text{Ni}$	8.35(45)	–	–
Ni-2	Hexanol 180 °C/24 h	NiFe_2O_4	8.34(07)	7.1±0.8	39.5

a Obtained by means of XRD.

b Obtained by means of TEM.

The crystal structure of the obtained materials was studied by X-ray powder diffraction (XRD) in a Siemens D-5000 diffractometer at room temperature and using Cu$K\alpha$ radiation (λ=1.5418 Å). The X-ray diffraction patterns were obtained in the 2θ range of 20°–80° and then were inspected using Match software [53] to identify the present crystallographic phases. The morphology and the microstructure of the samples were tested by scanning electron microscopy (SEM) in a JEOL 6400 microscope, by transmission electron microscopy (TEM) in a JEOL 1010 microscope operating at 100 kV and by high-resolution transmission electron microscopy (HRTEM) in a JEOL

2010 microscope operating at 200 kV. For TEM observations we have used suspensions of the ferrites obtained after ethanol washes, which were deposited onto the copper grids. The elemental composition of the samples was tested by energy-dispersive X-ray spectroscopy (EDS) with an Oxford Inca Energy 200 attached to the electronic microscope. Magnetic properties were studied in a DMS-1660 vibrating sample magnetometer (VSM) at room temperature varying the magnetic field up to ±10 kOe.

3. Results and discussion

XRD analysis shows that in all cases we have obtained crystalline MFe$_2$O$_4$ samples with the expected cubic spinel structure, identified as MnFe$_2$O$_4$ (JCPDS No. 01-075-0035), CoFe$_2$O$_4$ (JCPDS No. 00-022-1086) and NiFe$_2$O$_4$ (JCPDS No. 01-086-2267). As a resume, Table 1 summarizes the crystalline phases and the cell parameters obtained by XRD for the samples prepared under different synthesis conditions. As an example, we show in Fig. 1 the XRD patterns of MFe$_2$O$_4$ (M=Mn, Co, Ni) samples obtained from the reactions at 180 °C over a period of 24 h in the autoclave. The lattice constants calculated from (311) reflections are 8.52, 8.39 and 8.34 Å, for MnFe$_2$O$_4$, CoFe$_2$O$_4$ and NiFe$_2$O$_4$, respectively. A detailed analysis of the XRD results reveals that all the samples are single phased, with the exception of the sample Ni-1 (nominal NiFe$_2$O$_4$, synthesized in benzyl alcohol). In the XRD pattern of that sample we observe the presence of extra peaks, marked with arrows in Fig. 1(c), which correspond to the diffraction of metallic Ni with cubic structure (JCPDS No. 00-065-2865). We attributed the presence of metallic nickel to the reducing power of benzyl alcohol, which is able to reduce part of the Ni^{2+} to the Ni^0 form [54]. However, through substituting benzyl alcohol with hexanol, an alcohol with a lower reducing power, and maintaining the rest of the reaction conditions, we have obtained the desired NiFe$_2$O$_4$ phase (see Fig. 1(f)). Another interesting feature of the XRD patterns is the effective line broadening observed for all the samples, indicating the fine nature of the nanoparticles.

Fig. 1. XRD patterns of: (a) $MnFe_2O_4$, (b) $CoFe_2O_4$ and (c) $NiFe_2O_4$, synthesized in benzyl alcohol at 180 °C/24 h; (d) $MnFe_2O_4$, (e) $CoFe_2O_4$ and (f) $NiFe_2O_4$, synthesized in hexanol at 180 °C/24 h.
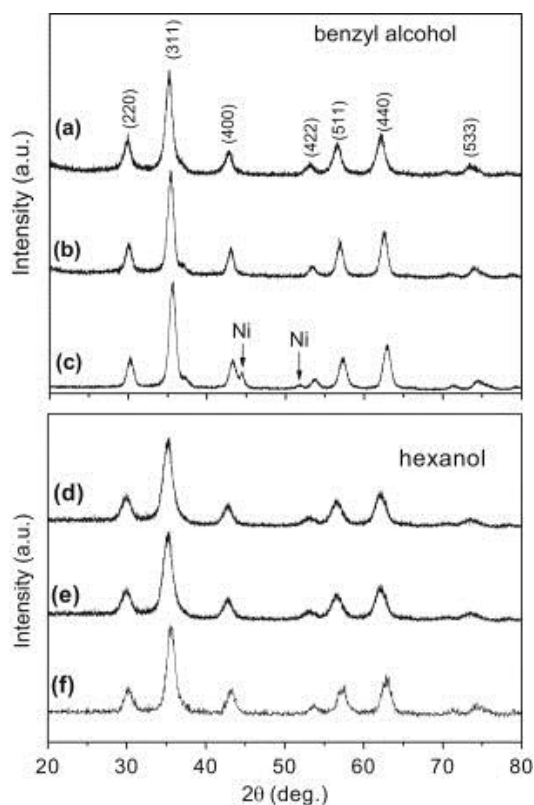
The morphology of the particles was studied in more detail by TEM, which reveals that we have obtained nanoparticles with spherical-like morphology and uniform sizes, ranging from 5 to 9 nm. In Fig. 2 and Fig. 3 we show some representative TEM micrographs of the ferrite nanoparticles obtained under different synthesis conditions; in Table 1 we summarize the average grain size deduced from TEM results for all the samples.

Comparing the ferrite samples that contain different metal cations, but prepared in similar synthetic conditions (see samples Mn-2, Co-4 and Ni-2 in Table 1 and in Fig. 2(a)–(c)), we observe a tendency of the particle size to increase when the ionic radii of the transition metal cation decreases.

Another interesting observation is the increase of the particle size with the reaction time. For example, $CoFe_2O_4$ nanoparticles obtained after reaction times of 24 h (sample Co-1) and 48 h (sample Co-2)—while maintaining unchanged the rest of the synthesis conditions—exhibit uniform sizes of 7.6±0.8 and 8.9±0.6 nm, respectively. However, when the reaction temperature was increased from 180 to 190 °C, the size of the nanoparticles did not appreciably changed, as we observe for Co-1 and Co-3 samples (see Table 1).
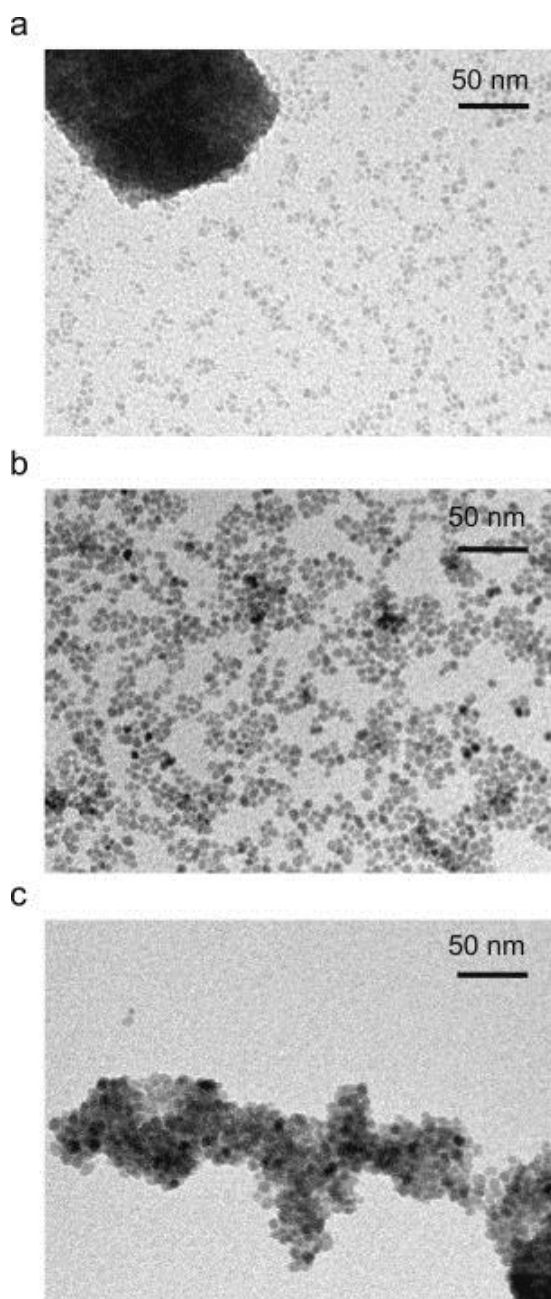
Fig. 2. TEM micrographs of: (a) $MnFe_2O_4$, (b) $CoFe_2O_4$ and (c) $NiFe_2O_4$ synthesized in hexanol at 180 °C/24 h.

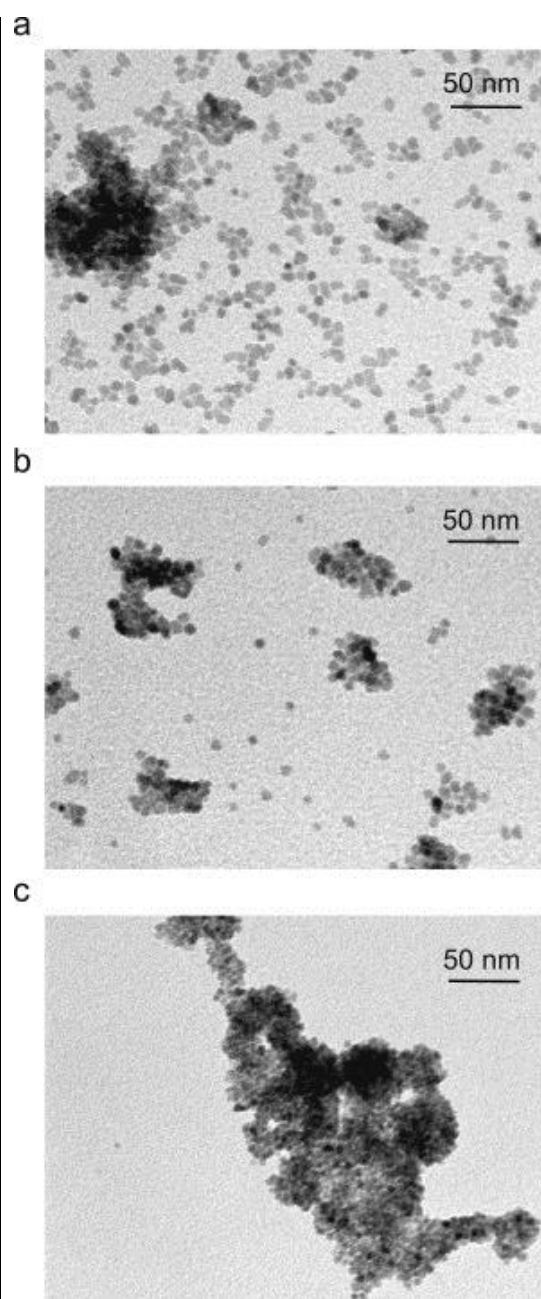Fig. 3. TEM micrographs of $CoFe_2O_4$ prepared in benzyl alcohol at: (a) 180 °C/24 h, (b) 190 °C/24 h and (c) 180 °C/48 h.

One of the most interesting results concerning this synthesis is the influence of the solvent on the size and agglomeration of the particles. We have observed through TEM that hexanol leads, in general, to the formation of slightly smaller ferrite particles than does benzyl alcohol. For example, as we can see in Table 1 and Fig. 2 and Fig. 3, $MnFe_2O_4$ nanoparticles with a diameter of 5.0±0.8 nm were obtained using hexanol. However, using benzyl alcohol in similar conditions, we obtain particles of 7.4±0.8 nm.

Similarly, we have prepared $CoFe_2O_4$ nanoparticles of 5.9±0.6 nm using hexanol, but nanoparticles of 7.6±0.8 nm using benzyl alcohol. The different broadening in XRD patterns confirms these TEM results: the line broadening in XRD patterns is higher for the ferrites prepared with hexanol (Fig. 1(d)–(f)) compared with the analogous samples prepared with benzyl alcohol (Fig. 1(a)–(c)). To explain these results, we have to consider the reaction mechanism in this solvothermal synthesis. This mechanism should be similar to that recently reported for the reaction of Fe(*acac*)$_3$ in benzyl alcohol to yield magnetite nanocrystals [52]: the main reaction occurs upon solvothermal treatment, involving solvolysis of the acetylacetonate, followed by aldol condensation reactions. In the first step, benzyl alcohol nucleophilically attacks one carbonyl group of the acetylacetonate ligand. In our case, the higher Lewis basicity of hexanol— compared with benzyl alcohol—enhances the solvolysis of the transition metal acetylacetonate species. As a consequence, the nucleation-reaction is faster and favoured with respect to the growth-reaction, and leads to the formation of smaller nanoparticles when using hexanol rather than benzyl alcohol.

Furthermore, we have observed appreciable differences in the stability of the ferrite suspensions prepared in hexanol compared to those prepared in benzyl alcohol. In general, the suspensions of the particles in hexanol remain stable for several days without precipitation, being more stable than the analogous in benzyl alcohol, which precipitate in minutes or hours. The clearest example is the case of the $CoFe_2O_4$ nanoparticles, whose suspensions in hexanol are stable for more than one week, while the corresponding suspensions in benzyl alcohol precipitate in less than one day.

The HRTEM images of the prepared particles indicate that the nanoparticles were structurally uniform and display good crystallinity. As an example, Fig. 4 shows a representative image of the $CoFe_2O_4$ particles (sample Co-1). The Fourier transform of the HRTEM image shows the electron diffraction pattern, which indicates that this particle is oriented along the [011] zone axis (see inset of Fig. 4). The interplanar distance of 8.3 Å indicated in Fig. 4 corresponds to the *a*-lattice parameter of the spinel structure, in agreement with the DRX results for $CoFe_2O_4$ particles. It is important to point out the good crystallinity of the particles, even near their surface, since this consideration plays an important role in their magnetic properties.

Fig. 4. High resolution transmission electron microscopy (HRTEM) image of $CoFe_2O_4$ prepared in benzyl alcohol at 180 °C/24 h. Inset: the Fourier transform of the HREM image shows the electron diffraction pattern, which indicates that this particle is oriented along the zone axis [011].
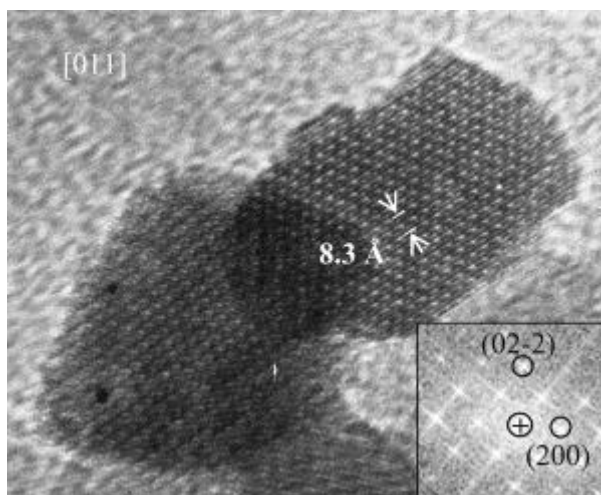
Results from EDS, performed on a scanning electronic microscope, in different regions of the products, show that Co/Ni/Mn, Fe and O were the main elemental components of the ferrite particles. These results also confirm the composition uniformity of the nanoparticles and the expected M:Fe atomic ratio, approximately equal to 1:2. More detailed EDS analysis performed on a transmission electron microscope confirm the presence of Mn/Co/Ni and Fe cations in individual particles. As an example, we show in Fig. 5 the EDS spectra obtained for the $CoFe_2O_4$ nanoparticles of Fig. 4.
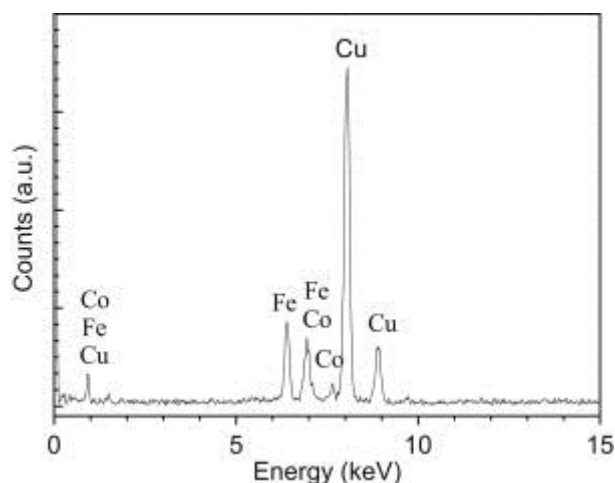

Fig. 5. EDS of $CoFe_2O_4$ particles prepared in benzyl alcohol at 180 °C/24 h.

Field-dependent magnetization of the synthesized nanoparticles was measured at room temperature (300 K), and by varying the magnetic field up to ±10 kOe. Fig. 6 and Fig. 7 display the field-dependent magnetization curves obtained for several representative samples. In Fig. 6 we show the hysteresis loops measured for three MFe_2O_4 samples (M=Mn, Co, Ni) which have similar particle size (φ~7 nm), while Fig. 7 compares the magnetic behaviour of three $CoFe_2O_4$ ferrite samples with

different particle sizes. In addition, the values of the magnetization at a maximum field of +10 kOe for all the samples are summarized in Table 1.

Fig. 6. Field-dependent magnetization measurements at RT of MFe_2O_4 (M=Co, Ni, Mn) ferrites with particle diameter ~7 nm.
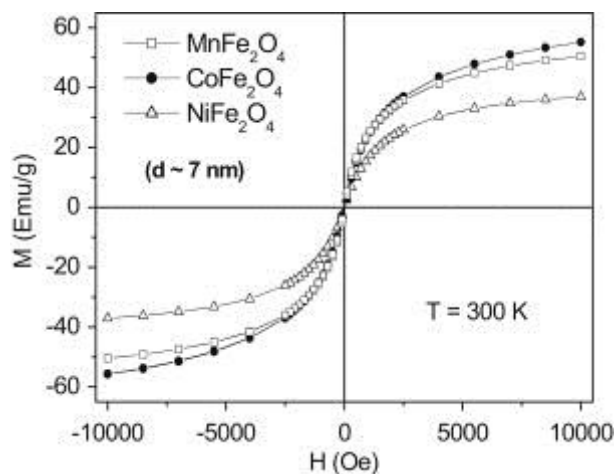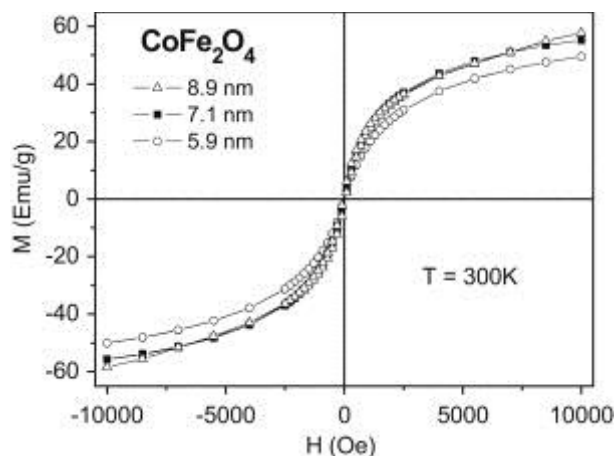

Fig. 7. Field-dependent magnetization measurements at RT of $CoFe_2O_4$ ferrites with different particle sizes.

All these measurements indicate that the ferrites exhibit superparamagnetic behaviour, as was expected for particles smaller than 10 nm [16] and [18]. We can also observe that the magnetization rises as the applied field increases, and reaches almost saturation point near the maximum applied field (±10 kOe).

Comparing samples that have different particle sizes, for example all the $CoFe_2O_4$ samples, we observe magnetization values of $M_{10 \text{ kOe}}$=58.4, 56.6, 55.4 and 50.2 emu/g for particles with diameters of 8.9, 7.6, 7.1 and 5.9 nm, respectively, which means a clear correlation between the decrease of the saturation magnetization and the decrease of the particle size, as was expected for these superparamagnetic particles [18] and [55]. These results confirm the capacity to control the magnetic properties of the nanoparticles by means of a simple variation of the solvothermal synthesis conditions.

All maxima magnetization for the prepared samples were very different to the reported values of the saturation magnetization for bulk ferrites (~80 emu/g) [52], as was expected for particles much smaller than the single domain size (~70 nm) [16]. However, the maxima magnetization of our particles are comparable, or even higher, to those reported for superparamagnetic ferrite nanoparticles prepared using another different methods and with similar particle sizes [19], [20], [21], [24], [26], [33], [48] and [49]. We have to take into account that the magnetic properties of such small nanoparticles are highly dependent on the surface effects (i.e. spin-canting [25]), that become more dominant as the size of the particles are smaller[25]. The achieved values of the maxima magnetization of these nanoparticles are related to their crystallinity, even near their surface.

4. Conclusions

We have confirmed that the previously described solvothermal method for the synthesis of Fe_3O_4 can also be adapted to prepare another MFe$_2$O$_4$ ferrites (M=Mn, Co and Ni). The most important advantage of this method is that it provides a one step, simple, general and inexpensive method for the preparation of ferrite nanoparticles at low synthesis temperature. In that synthesis, an alcohol is used both as a solvent and a ligand, avoiding the use of surfactants and simplifying the preparation of dispersed particles. The adequate choice of the synthesis conditions (i.e. transition metal cations, alcohol, reaction temperature and reaction time) allow us to obtain stable suspensions of monodispersed particles of MFe$_2$O$_4$ (M=Mn, Co and Ni), with diameters ranging from 5 to 10 nm, and with good crystallinity. As solvent we have used benzyl alcohol and, by first time, hexanol. In the case of the synthesis of $NiFe_2O_4$, this ferrite could be easily prepared using hexanol; however, benzyl alcohol is not an adequate solvent, because it partially reduces the Ni^{2+}cation to Ni^0. In general, hexanol seems to be more adequate as a solvent for the synthesis of the oxides of last transition metal cations (i.e. nickel) without the reduction. Moreover, this solvent allows the synthesis of smaller particles and more stable suspensions than benzyl alcohol.

The hysteresis loops of these ferrites, measured at room temperature and under maximum applied field of 10 kOe, shows their superparamagnetic behaviour, as was expected for single domain nanoparticles. The maxima magnetization for the MFe$_2$O$_4$ ferrites is quite interesting for such small nanoparticles, and is due to the

high crystallinity of the obtained samples. The synthesis conditions are demonstrated to have a clear influence on their saturation magnetization.

Acknowledgments

References

1. F. Caruso, M. Spasova, A. Susha, M. Giersig, R.A. Caruso

    Chem. Mater., 13 (2001), pp. 109–116

2. T. Hyeon

    Chem. Commun., 8 (2003), pp. 927–934

3. Y. Xiong, X. Xie, S. Chen, Z. Li

    Chem. Eur. J., 9 (2003), pp. 4991–4996

4. Yu, M. Mizuno, Y. Sasaki, H. Kondo

    Appl. Phys. Lett., 81 (2002), pp. 3768–3771

5. M. Schaefer, G. Dietzmann, H. Writh

    J. Magn. Magn. Mater., 101 (1991), pp. 95–96

6. S. Yu, M. Yoshimura

    Chem. Mater., 12 (2000), pp. 3805–3810

7. C.R. Vestal, Z.J. Zhang

    J. Am. Chem. Soc., 125 (2003), pp. 9828–9833

8. S. Sun, H. Zeng, D.B. Robinson, S. Raoux, P.M. Rice, S.X. Wang, G. Li

    J. Am. Chem. Soc., 126 (2004), pp. 273–279

9. X. Jia, D. Chen, X. Jiao, T. He, H. Wang, W. Jiang

    J. Phys. Chem. C, 112 (2008), pp. 911–917

10. P. Tartaj

Curr. Nanosci., 2 (2006), pp. 43–53

11. T.J. Daos, G. Pourroy, S. Bejín-Colin, J.M. Grenèche, C. Ulhag-Boiullet, P. Legaré, P. Bernhardt, C. Leuvrey, G. Rogez

    Chem. Mater., 18 (2006), pp. 4399–4404

12. H.M. Lu, W.T. Zheng, Q. Jiang

    J. Phys. D: Appl. Phys., 40 (2007), pp. 320–325

13. H.B. Na, I.C. Song, T. Hyeon

    Adv. Mater., 21 (2009), pp. 1–16

14. S.G. Grancharov, H. Zeng, S. Sun, S.W. Wang, S. O'Brien, C.B. Murray, J.R. Kirtley, G.A. Held

    J. Phys. Chem. B, 109 (2005), pp. 13030–13035

15. Q. Song, Z.J. Zhang

    J. Phys. Chem. B, 110 (2006), pp. 11205–11209

16. Berkowitz, W.T. Schuele

    J. Appl. Phys., 30 (1959), pp. 134S–135S

17. R.M. Cornell, U. Schwertmann

    The Iron Oxides. Structure, Properties, Reactions, Occurrences and Uses

    Wiley-VCH, Weinheim (2003)

18. A.F. Rebolledo, A.B. Fuertes, T. González-Carreño, M. Sevilla, T. Balde-Solis, P. Tartaj

    Small, 4 (2008), pp. 254–261

19. Hu, Z. Gao, X. Yang

    J. Magn. Magn. Mater., 320 (2008), pp. L70–L73

20. Q. Song, Y. Ding, Z.L. Wang, Z.J. Zhang

    Chem. Mater., 19 (2007), pp. 4633–4638

21. Liu, B. Zou, A.J. Rondinone, Z.J. Zhang

    J. Am. Chem. Soc., 122 (2000), pp. 6263–6267

22. Antic, A. Kremenovic, A.S. Nikolic, M. Stoiljkovic

    J. Phys. Chem. B, 108 (2004), pp. 12646–12651

23. N.S. Gajbhiye, G. Balaji, M. Ghafari

    Phys. Stat. Sol. A, 189 (2002), pp. 357–361

24. X. Jia, D. Chen, X. Jiao, T. He, H. Wang, W. Jiang

J. Phys. Chem. C, 112 (2008), pp. 911–917

25. M.P. Morales, S. Veintenillas-Verdaguer, M.I. Montero, C.J. Serna, A. Roig, L. Casas, B. Martínez, F. Sandiumenge

    Chem. Mater., 11 (1999), pp. 3058–3064

26. C.R. Vestal, Z.J. Zhang

    Int. J. Nanotechnol., 1 (2004), pp. 240–263

27. C.N. Chinnasamy, M. Senote, B. Jeyadevan, O. Perales-Perez, K. Shinoda, K. Tohji

    J. Colloid Interface Sci., 263 (2003), pp. 80–83

28. O. Masala, R. Seshadri

    Chem. Phys. Lett., 402 (2005), pp. 160–164

29. Z. Xu, C. Shen, Y. Hou, H. Gao, S. Sun

    Chem Mater., 21 (2009), pp. 1778–1780

30. J.G. Lee, H.M. Lee, C.S. Kim, Y.G. Oh

    J. Magn. Magn. Mater., 177 (1998), pp. 181–182

31. V. Pillai, D. Shah

    J. Magn. Magn. Mater., 163 (1996), pp. 243–248

32. K. Maaz, A. Mumtaz, S.K. Hasanain, A. Ceylan

    J. Magn. Magn. Mater., 308 (2007), pp. 289–295

33. Y. Qu, H. Yang, N. Yang, Y. Fan, H. Zhu, G. Zou

    Mater. Lett., 60 (2006), pp. 3548–3552

34. Manova, B. Kunev, D. Paneva, I. Mitov, L. Petrov, C. Estournes, C. D'Orleans, J.L. Rehspringer, M. Kurmoo

    Chem. Mater., 16 (2004), pp. 5689–5696

35. R. Sani, A. Beitollahi, Y.V. Maksimov, I.P. Suzdalez

    J. Mater. Sci., 42 (2007), pp. 2126–2131

36. Liu, B. Zou, A.J. Rondinone, Z.J. Zhang

    J. Phys. Chem. B, 104 (2000), pp. 1141–1145

37. M. Bellusci, S. Canepari, G. Ennas, A. La Barbera, F. Padella, A. Santini, A. Scano, L. Seralessandri, F. Varsano

    J. Am. Ceram. Soc., 90 (2007), pp. 3977–3983

38. Bilecka, I. Djerdj, M. Niederberger

Chem. Commun., 7 (2008), pp. 886–888

39. W.C. Hsu, S.C. Chen, P.C. Kuo, C.T. Lie, W.S. Tsai

   Mater. Sci. Eng. B, 111 (2004), pp. 142–149

40. R. Saez Puche, M.J. Torralvo Fernandez, V. Blanco Gutierrez, R. Gomez, V. Marquina, M.L. Marquina, J.L. Perez Mazariego, R. Ridaura

   Bol. Soc. Esp. Ceram., 47 (2008), pp. 133–137

41. S. Si, C. Li, X. Wang, D. Yu, Q. Peng, Y. Li

   Cryst. Growth Des., 5 (2005), pp. 391–393

42. Y. Hou, J. Yu, S. Gao

   J. Mater. Chem., 13 (2003), pp. 1983–1987

43. A.R. Gainsford, M.J. Sisley, T.W. Swaddle

   Can. J. Chem., 53 (1975), pp. 12–19

44. H. Kumazawa, K. Oki, H.M. Cho, E. Sada

   Chem. Eng. Commun., 115 (1992), pp. 25–33

45. K.J. Davies, S. Wells, R.V. Upadhyly, S.W. Charles, K.O. Grady, M. El Hilo, T. Meaz, S. Morup

   J. Magn. Magn. Mater., 149 (1995), pp. 14–18

46. Rabenau

   Angew. Chem. Int. Ed., 24 (1985), pp. 1026–1040

47. S. Komarneni, M.C. D'Arrigo, C. Leonelli, G.C. Pellacani, H. Katsuki

   J. Am. Ceram. Soc., 81 (1998), pp. 3041–3043

48. H. Deng, X. Li, Q. Peng, X. Wang, J. Chen, Y. Li

   Angew. Chem. Int. Ed., 44 (2005), pp. 2782–2785

49. H. Deng, H. Chen, H. Li

   Mat. Chem. Phys., 11 (2007), pp. 509–513

50. S. Sun, H. Zeng

   J. Am. Chem. Soc., 124 (2002), pp. 8204–8205

51. N. Pinna, S. Grancharov, P. Beato, P. Bonville, M. Antonietti, M. Niederberger

   Chem. Mater., 17 (2005), pp. 3044–3049

52. M. Niederberger, G. Garnweitner

   Chem. Eur. J., 12 (2006), pp. 7282–7302

53. 〈http://www.crystalimpact.com〉.

54. F.L. Jia, L.Z. Zhang, X.Y. Shang, Y. Yan

    Adv. Mater., 20 (2008), pp. 1050–1054

55. J. Smith, H.P.J. Wijn

    Ferrites. Physical Properties of Ferromagnetic Oxides in Relation to their Technical Applications

    Wiley, New York (1959)